

Document downloaded from:

<http://hdl.handle.net/10251/48740>

This paper must be cited as:

Verdú Martín, GJ.; Juste Vidal, BJ.; Miró Herrero, R. (2012). Uncertainty and sensitivity analysis of the effect of the mean energy and FWHM of the initial electron fluence on the Bremsstrahlung photon spectra of linear accelerators. *Applied Radiation and Isotopes*. 70(7):1267-1271. doi:10.1016/j.apradiso.2012.03.040.



The final publication is available at

<http://dx.doi.org/10.1016/j.apradiso.2012.03.040>

Copyright Elsevier

Uncertainty and sensitivity analysis of the effect of the mean energy and FWHM of the initial electron fluence on the Bremsstrahlung photon spectra of linear accelerators

B. Juste^{1*}, R. Miró¹, G. Verdú¹, R Macián²

¹The Institute for Industrial, Radiophysical and Environmental Safety (ISIRYM),

Universitat Politècnica de València, Camí de Vera s/n 46022 València, Spain

²Lehrstuhl für Nukleartechnik, Technical University Munich, Germany.

Abstract. A calculation of the correct dose in radiation therapy requires an accurate description of the radiation source because uncertainties in characterization of the linac photon spectrum are propagated through the dose calculations. Unfortunately, detailed knowledge of the initial electron beam parameters is not readily available, and many researchers adjust the initial electron fluence values by trial-and-error methods. The main goal of this work was to develop a methodology to characterize the fluence of initial electrons before they hit the tungsten target of an Elekta Precise medical linear accelerator. To this end, we used a Monte Carlo technique to analyze the influence of the characteristics of the initial electron beam on the distribution of absorbed dose from a 6 MV linac photon beam in a water phantom. The technique is based on calculations with Software for Uncertainty and Sensitivity Analysis (SUSA) and Monte Carlo simulations with the MCNP5 transport code. The free parameters used in the SUSA calculations were the mean energy and full-width-at-half-maximum (FWHM) of the initial electron distribution. A total of 93 combinations of these parameters gave initial electron fluence configurations. The electron spectra thus obtained were used in a simulation of the electron transport through the target of the linear accelerator, which produced different photon (Bremsstrahlung) spectra. The simulated photon spectra were compared with the 6-MV photon spectrum provided by the linac manufacturer (Elekta). This comparison revealed how the mean energy and FWHM of the initial electron fluence affect the spectrum of the generated photons.

*Corresponding autor: Belén Juste. bejusvi@iqn.upv.es

Tel: 0034 963879631

Fax: 0034 963877639

This study has made it possible to fine-tune the examined electron beam parameters to obtain the resulted absorbed doses with acceptable accuracy (error <1%).

Keywords: uncertainty and sensitivity analysis; Monte Carlo methods; MCNP5; Elekta radiotherapy linac, electron spectrum.

1. Introduction

Precise Monte Carlo treatment planning systems simulate particle transport from the tungsten target to the patient. For accurate dose calculations, characteristics of the electron beam hitting the target, as well as the particle transport through the whole unit head, need to be modeled accurately.

Detailed parameters of the initial electron beam are not readily available, and researchers usually adjust the initial electron fluence values by trial-and-error methods. Accelerated in the waveguide, electrons impinge on the tungsten target to generate a Bremsstrahlung photon treatment beam. Errors in the description of the incident electron fluence may affect the estimated dose received by the patient. ICRU 24 (1976) recommends that the maximal error in a treatment planning dose calculation would not exceed 2% of the prescribed dose. This error includes many contributions, such as errors in the geometry model, physics parameters, and also in characteristics of the radiation source, on which this work is focused.

One of the most comprehensive studies of Monte Carlo modeling of linear accelerators was performed by Sheikh-Bagheri and Rogers (Sheikh-Bagheri and Rogers, 2002a), who studied sensitivity of the photon beam simulations to the parameters of the initial electron fluence. They concluded that two most important parameters in simulating photon radiotherapy beams are the mean energy and the radial spread of the incident electron beam. These parameters were studied also in this work. The aim of our study was to find a distribution of the fluence of electrons incident on the target that, when transported through the treatment head and used in dosimetric calculations, can reproduce experimental doses in a water phantom within 1%. This paper also describes the effect of the uncertainty in the spectrum of the electrons hitting the tungsten target on the uncertainty of the spectrum of photon used in radiation therapy, which

was previously studied by other investigators (Tzedakis et al., 2004; Sheikh-Bagheri and Rogers, 2002b).

The first part of this work consisted of a Monte Carlo calculation for a source of a unidirectional electron beam with a Gaussian energy distribution specified by Elekta (mean energy 6.3 MeV; full width at half maximum, FWHM, 0.11 MeV). A Best Estimate Analysis (BEA) (Crow, 1960; Guba, 2003) performed in this work consisted of a description of the mean and FWHM of the electron energy; uncertainties in both the parameters were included in the analysis and jointly propagated. The statistically-based BEA performs a Monte Carlo sampling of the uncertainty of the mean and FWHM of an electron energy spectrum. The size of the sampling is determined from the characteristics of the tolerance intervals by applying the Noether-Wilks formulas (Wilks, 1962). In the 93 simulations performed, the mean energy and FWHM were directly modified according to the uncertainty. Once the results of the 93 cases were obtained, a non-parametric statistical method was applied to the resulted photon spectra to determine their tolerance intervals. It is well known that the resulted photon spectra are affected by uncertainties of several types, with the biggest effect of the uncertainty in the electron energy spectrum. Therefore, it was necessary to apply uncertainty propagation techniques to quantify the uncertainty of the photon spectrum estimation. In this work, we present an uncertainty and sensitivity analysis (McKay, 1988) of the energy spectrum of initial electrons in an Elekta linac.

2. Materials and methods

2.1. Methodology of the uncertainty and sensitivity analysis

The BEA method of sensitivity analysis can provide a posteriori assessment of the importance of the input parameters. An advantage of the methodology based on a statistical sample of input variables and code models is that there is no need to decide a priori which of the input variables

are more important for the simulation. The first step in this methodology is to identify the relevant input variables and code models. The relevant input variables considered in this work are based on the studies by Sheikh-Bagheri and Rogers (Sheikh-Bagheri and Rogers, 2002a). They are mean electron energy M and electron energy full width at half maximum, $FWHM$.

2.1.1. Description of the model

According to Elekta, the electron spectrum has a Gaussian distribution with the mean 6.3 ± 0.3 MeV and $FWHM$ 0.11 ± 0.03 MeV (Elekta, 2006). Distributions of the electron energy and the electron radial intensity are both assumed to be Gaussian. The electron energy spread, characterized by $FWHM$, was taken as specified by the manufacturer. The modeled electron beams were incident normal to the target and had no divergence.

Using these parameters, we performed an MCNP5 (Los Alamos National Laboratory, 2003) simulation of the electron beam transport from the linac waveguide to the tungsten target. The tungsten alloy target (10% Re, 90% W, 19.49 g/cm^3) is a disc, and its complete geometry was modeled in detail according to the manufacturer's specifications (Juste et al., 2007).

Each Monte Carlo simulation was run until the uncertainty in the computed fluences or depth-dose curves went down to below 0.3%, which corresponded to $1 \cdot 10^9$ simulated histories (nps).

Fig. 1 shows a Bremsstrahlung spectrum simulated from the initial electron spectrum.

To validate the photon spectrum thus obtained, we used it to simulate a depth-dose curve for a water phantom. A simulation of the whole unit is required when a calculated spectrum needs to be validated.

To simulate the transport of electrons and photons through the unit, from the source to the detector in a water phantom, we realistically modelled the geometry of all the involved components. The accelerator head was represented by the target disc, primary collimators, flattening filter, the monitor ionization chamber assembly, and the auto-wedge assembly, which included the wedge and the backscatter plate. All dimensions and material specifications were taken from the Elekta documentation. A schematic diagram in Fig. 2 shows the MCNP5 geometric model of the typical upper head configuration for low-energy photon beams (Juste et al., 2010; Juste et al., 2011; U.S. Environmental Protection Agency, 2001).

The simulations used the 6 MV photon spectrum shown in Fig. 1. The photon source was at 100 cm from the surface of the water phantom ($50 \times 50 \times 50 \text{ cm}^3$), and the field size was $10 \times 10 \text{ cm}^2$. The FMESH4 tally (Los Alamos National Laboratory, 2003) with the corresponding flux-to-dose conversion factors were used to obtain doses in the water phantom. The FMESH card makes it possible to define a mesh tally superimposed on the problem geometry and to estimate lengths of the tracks of the particle flux. By default, this tally is averaged over a mesh cell, in units of particles/cm². Therefore, this card was used in combination with the dose energy (DE) and dose function (DF) cards to transform the output results into doses in Gy.

Fig. 3 shows the simulated and an experimental depth-dose curves normalized to the maximal doses. The experimental curve was obtained with an Elekta Precision linac at the Hospital Clínic Universitari de València. The root mean square difference between the curves in the deeper region is approximately 5%.

The initially used electron spectrum could not reproduce the experimental curve exactly because of the spectrum variations within the manufacturer's tolerances. Therefore, an uncertainty analysis was needed in order to find a range where the photon spectrum emitted by the linac is located with 95% sureness.

2.2. Uncertainty analysis

In the uncertainty analysis, the input parameters (mean energy and FWHM) were assumed to be random values from the ranges of their variation, which needed to be found experimentally or taken from previous experience. Probability density functions (PDFs) were assigned to the input parameters before the sampling process. PDFs quantify the likelihood that the variables will have specific values within the ranges of their variation. This initial phase of the analysis was the most subjective step of the entire process.

A determination of PDFs is not a simple task, and the actual functions are not known for many variables. When no data are available, the only recourse is to assign subjective PDFs (SPDF) based on experience or subjective judgment. One of the most frequently used PDFs is the uniform distribution, which assigns equal probability to any value in the range of variation of the variable. Normal and lognormal distributions are commonly used to describe experimental measurements and other natural variations. They can also be truncated to account for the fact that some parameters may have their ranges of variation limited by physical constraints, such as minimal or maximal energy. The uniform PDF was chosen for both the mean energy and the FWHM.

After the PDFs and ranges of variation were assigned to the input variables and code models, the space of these random variables was sampled. The precision of the obtained results does not depend on the number of input parameters, but it depends, among other factors, on the sample

size and randomness of the sampling procedure. The minimal number of the sample or the code calculations (n) necessary for the desired precision is given by the Wilks' formula (Wilks, 1962). A statistical analysis of output variables (Y) _{N} with non-parametric methods can produce tolerance intervals, which are able to quantify the uncertainty of Y . A tolerance interval is an estimate of the interval of variability of a random variable that contains a specified fraction of the variable's probability, p , with a prescribed level of confidence, γ . Tolerance intervals were constructed from the sampled data so as to enclose $p\%$ of the population of a random variable Y with a given confidence $\gamma\%$. They show where most of the population of Y can be expected as the variable is affected by the uncertainty of the input parameters and physical and mathematical models.

The number of code calculations is independent of the number of input uncertainties; it depends only on the defined probability p and confidence level γ . The sample size is determined by the requirement to estimate the tolerance/confidence interval for the quantity of interest. Wilks' formula (Wilks, 1962) is used to determine the number of simulations necessary for the desired uncertainty bands:

$$\gamma = 1 - p^n - n(1-p)p^{n-1} \quad (1)$$

The upper statistical tolerance limits are the upper γ confidence for the chosen defined probability p . The sample size obtained with Wilks' formula for double tolerance limits with a 95% uncertainty and with 95% statistical confidence for the output variables was equal to 93.

The MCNP simulation was executed 93 times, each one with a different randomly chosen set of values of mean energy and FWHM sampled from the uniform distributions. Fig. 4 shows ten of the 93 input cases.

Electrons with the 93 random spectra were transported through the target by Monte Carlo simulation. Fig. 5 shows ten of the resulted simulated photon spectra.

As a result of describing the uncertainties in the input variables with probability distribution functions, the code output results are also random variables. PDFs of the photon spectra results would contain all the information needed to compute their uncertainties. The problem is that such functions are usually unknown. Therefore, in order to quantify the uncertainties exactly, one should generate the PDFs from the sampled output values. However, this is not always feasible. The only alternative is to obtain as much information about the PDF properties and main parameters as possible from simulated distribution functions and estimators.

In the uncertainty analysis, the main goal was to quantify the variability of the code output as a function of the variability in the inputs. If a random sample of output values $((Y)_1, \dots, (Y)_n)$ has a normal PDF, it is possible to compute tolerance intervals for sample mean m_y and sample standard deviation s_y . It is not easy to guarantee, however, that the sample of the output values is normally distributed. Nevertheless, if the sample is random, statistical tests for normality can be used to quantify how well the hypothesis of normality fits the sampled data. Three of these tests are the *W*-statistic (Zar, 1984), the Lilliefors test (Lilliefors, 1967) and the Kolmogorov's normality test (Zar, 1984). The Lilliefors test performed by SUSAS software on the photon spectra input data found them normally distributed; so, a two-sided tolerance interval could be calculated (Fig. 6).

Sheikh-Bagheri and Rogers (2002b) found that photon spectra are different for different energies and machines from different manufacturers. Fig. 7 shows that the spectrum obtained

by them for the Elekta 6 MV beam is within the 98% tolerance band calculated in this work. This validates the two-sided tolerance interval calculated by the SUSAs software.

Lower and upper tolerance limits would change if the uniform distribution was replaced with a normal one. Therefore, our future work will include normal distributions of these variables instead of the uniform ones because it will likely provide wider tolerance intervals.

We used the upper-limit and the lower-limit fluence spectra for the photon beam in two full Monte Carlo simulations of the complete linac head to obtain the corresponding depth-dose curves for a water phantom. These curves were compared with the experimental data. As Fig. 8 shows, the simulation based on the lower tolerance limit spectrum produced a depth-dose curve that agreed with the experimental data within 1% (a root mean square difference).

3.3. Sensitivity analysis

The purpose of our sensitivity analysis was to quantify the effect of the input variables on the depth-dose curves. Sensitivity measures can quantify this, and, thus, be useful for an a posteriori ranking of the importance of each of the input variables for the output variable of interest.

Most of the sensitivity measures are related to regression analysis. Some of them are useful to detect linear relationships, while others, like the so-called rank correlations (Iman, 1980), are useful to quantify relations between variables that behave monotonically with respect to each other (e.g., smooth variations of one variable correspond to smooth variations of the other). A comparison of these two types of measures applied to the same data set can detect non-linearity of the dependence of depth-dose curves on the studied parameters. Examples of linear measures are the simple correlation coefficient (SCC), or Pearson's moment product, and the

partial correlation coefficient (PCC). We used Pearson's moment product coefficients evaluated with the SUSAN software.

The Pearson's moment product coefficient is a measure of a correlation (linear dependence) between two variables, namely, electron spectrum distribution and photon spectrum distribution. Its value ranges between +1 and -1 inclusively and gives a measure of the strength of linear dependence between the two variables. Pearson's moment product coefficient between two variables is defined as the covariance of the two variables divided by the product of their standard deviations. A value of 1 implies that a linear equation describes the relationship between both variables perfectly, with all data points lying on a straight line showing increase of one variable with an increase of the other. A value of -1 implies that all data points lie on a straight line showing that one variable decreases as the other increases. A value of 0 implies that there is no linear correlation between the variables.

The scalar sensitivity analysis showed that the parameter of the electron beam most important for uncertainty of the delivered doses is FWHM, which displays a higher sensitivity value = 0.2 (Fig. 9). The uncertainty in the mean energy (sensitivity value = 0.15) appears to have a weaker effect on the output variables. Nevertheless, as the differences between these two parameters are not significant (lower than 10%), one can state that both the variables have similar influence on depth-dose curves. A value of 0.1 implies that there is only a weak linear correlation between the variables.

The depth-dose curves are almost as sensitive to the mean energy of the electron beam as to its energy spread, as can be seen in Fig. 9, because the sensitivity values of both parameters differ by less than 10%.

The least known parameters in a Monte Carlo simulation of a linear accelerator treatment head are often the properties of the initial electron beam directed onto the exit vacuum window. A total of 93 initial beams with different spatial fluence distributions have been transported through the geometry of a linac accelerator. The electron beam characteristics (energy spectrum distributions) and the subsequent relative absorbed dose distributions in a water phantom were calculated. The relationship between the electron energy spectral spread and the photon spectrum distribution is, however, small, as reported by Björk (2002).

REFERENCES

Björk, P., Knöös, T., Nilsson, P., 2002. Influence of initial electron beam characteristics on Monte Carlo calculated absorbed dose distributions for linear accelerator electron beams. *Phys Med Biol.* 47 (22), 4019-4041.

Crow, E. L., 1960. *Statistics Manual with Examples Taken from Ordnance Development.* Dover Publications, New York.

Elekta Limited, 2006. Information for Monte Carlo Modelling of the Elekta Linear Accelerator – Machine 5463 onwards. Confidential Information.

Guba, A., Makai, M., Pal, L., 2003. Statistical aspects of best estimate method - I, *Reliability engineering & system safety*, 80, 217-232.

ICRU Report 24, "Determination of Absorbed Dose in a Patient Irradiated by Beams of X or Gamma Rays in Radiotherapy", International Commission on Radiation Units and Measurements, 1976.

Iman, R.L., Davenport, J.M., 1980. Rank Correlation Plots for Use with Correlated Input Variables in Simulation Studies. Report No. SAND80, 1903. Sandia National Laboratories, Albuquerque, NM.

Juste, B., Mota, M.E., Miró, R., Gallardo, S., Verdú, G., 2007. Monte Carlo modeling of the Elekta precise linear accelerator: Validation of dose distribution in a heterogeneous water phantom. Joint Int. Topical Meeting on Mathematics & Computation and Supercomputing in

Nuclear Applications (M&C + SNA 2007). Monterey, California, April 15-19, 2007. (CD ROM)

Juste, B., Miró, R., Verdú, G., Díez, S., Campayo, J.M., 2010. Electron influence on the reconstruction of a linac 6 MeV photon spectra by unfolding methods. Conf. Proc. IEEE Eng. Med. Biol. Soc., 577-580.

Juste, B., Miró, R., Verdú, G., Díez, S., Campayo, J.M., 2011. Bremsstrahlung spectrum reconstruction from gradient depth dose curves obtained in a water phantom. Nucl. Technol. 175 (1), 175-181.

Lilliefors, H. W., 1967. On the Kolmogorov-Smirnov tests for normality with mean and variance unknown. J. Am. Statist. Association, 62 (318), 399-402.

McKay, M. D., 1988. Sensitivity and Uncertainty Analysis Using a Statistical Sample of Input Values. CRC Press, Boca Raton, FL.

Sheikh-Bagheri, D., Rogers, D. W. O., 2002. Monte Carlo calculation of nine megavoltage photon beam spectra using the BEAM code. Med. Phys. 29 (3), 391-402.

Sheikh-Bagheri, D., Rogers, D. W. O., 2002. Sensitivity of megavoltage photon beam Monte Carlo simulations to electron beam and other parameters. Med Phys. 29 (3), 379-390.

Tzedakis, A., Damilakis, J.E., Mazonakis, M., Stratakis, J., Varveris, H., Gourtsoyiannis, N., 2004. Influence of initial electron beam parameters on Monte Carlo calculated absorbed dose distributions for radiotherapy photon beams. Med Phys. 31 (4), 907-913.

U.S. Environmental Protection Agency, 2001. Risk Assessment Guidance for Superfund: Volume III - Part A. Process for Conducting Probabilistic Risk Assessment. Office of Emergency and Remedial Response U.S. Environmental Protection Agency Washington, DC.

Wilks S. S., 1962. Mathematical Statistics. Wiley, New York.

Los Alamos National Laboratory, 2003. X-5 Monte Carlo Team, MCNP – A General Monte Carlo N Particle Transport Code, Version 5”, LA-UR-03-1987.

Zar, J. H., 1984. Biostatistical Analysis. 2nd ed. Prentice-Hall, Englewood Cliffs, NJ.

Captions to Figures

Fig. 1. A Bremsstrahlung spectrum obtained by an MCNP5 simulation from the electron spectrum with the mean energy of 6.3 MeV and FWHM of 0.11 MeV.

Fig. 2. A diagram of the Elekta Precise unit head modeled with the MCNP5 code.

Fig. 3. Simulated and experimental depth-dose curves for 6 MV photons (mean energy 6.3 MeV; FWHM 0.11 MeV).

Fig. 4. Selected randomly generated distributions of the electron beam spectrum.

Fig. 5. Selected photon spectra obtained by the simulation.

Fig. 6. Tolerance limits for the simulated photon spectra (93 cases).

Fig. 7. Energy spectrum of the 6 MV photon beam of Elekta linac (Sheikh-Bagheri and Rogers, 2002a) compared with the tolerance band obtained in this work.

Fig. 8. Experimental and calculated depth-dose curves for an Elekta 6 MV photon beam.

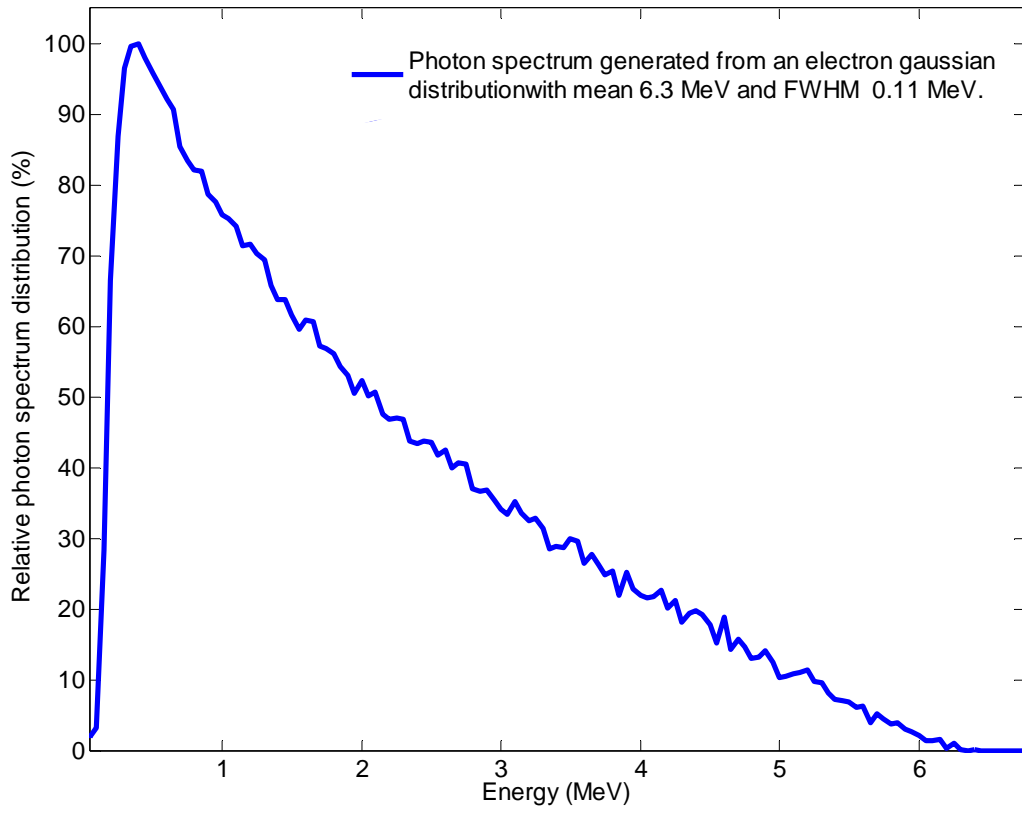


Fig. 1.

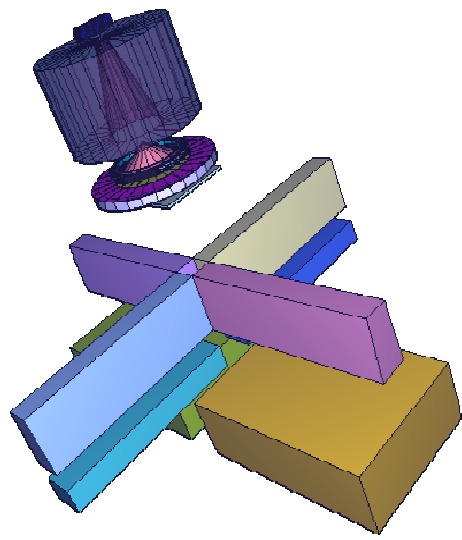


Fig. 2.

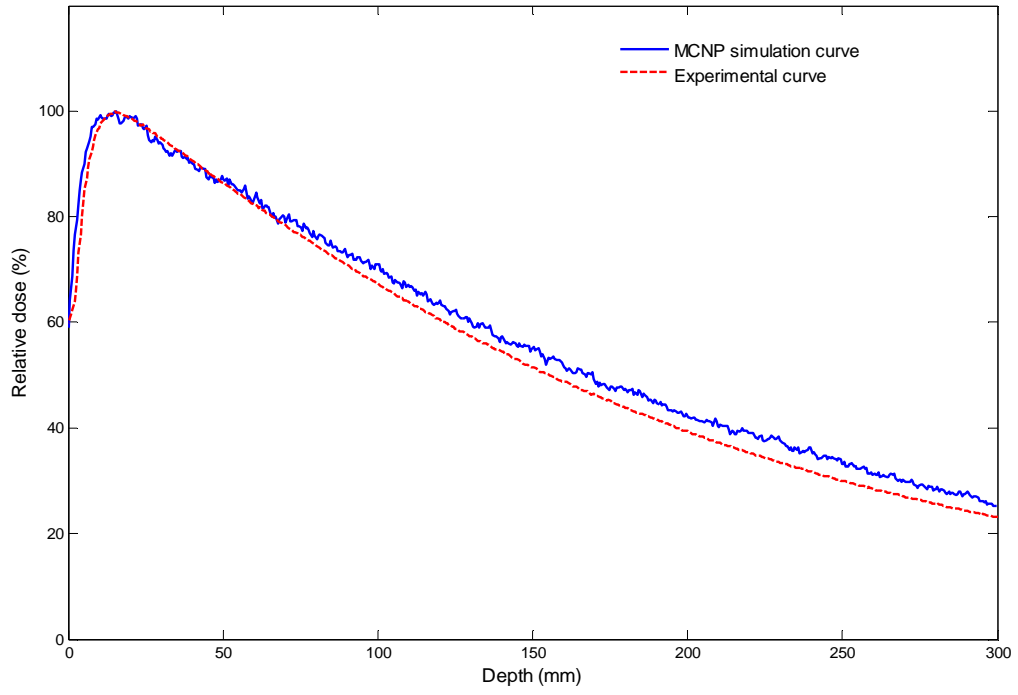


Fig. 3.

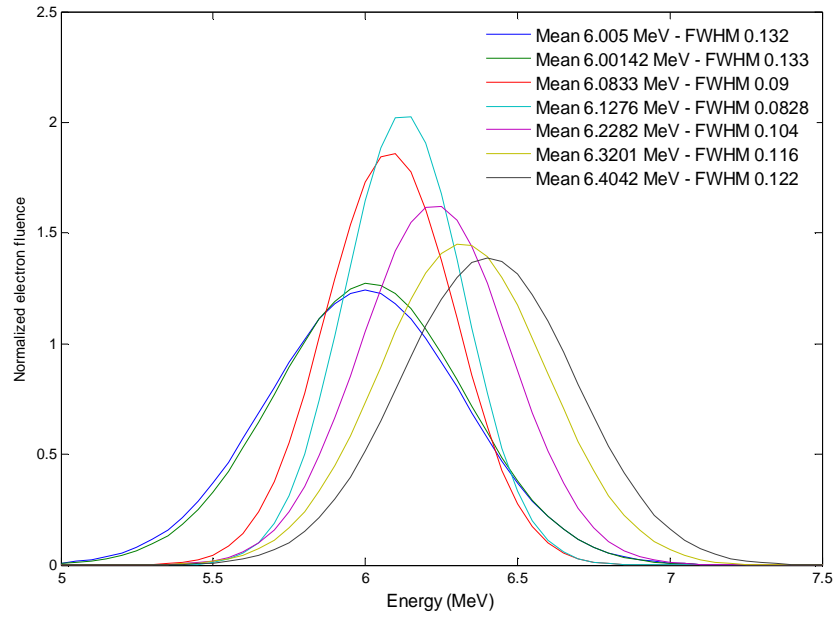


Fig. 4.

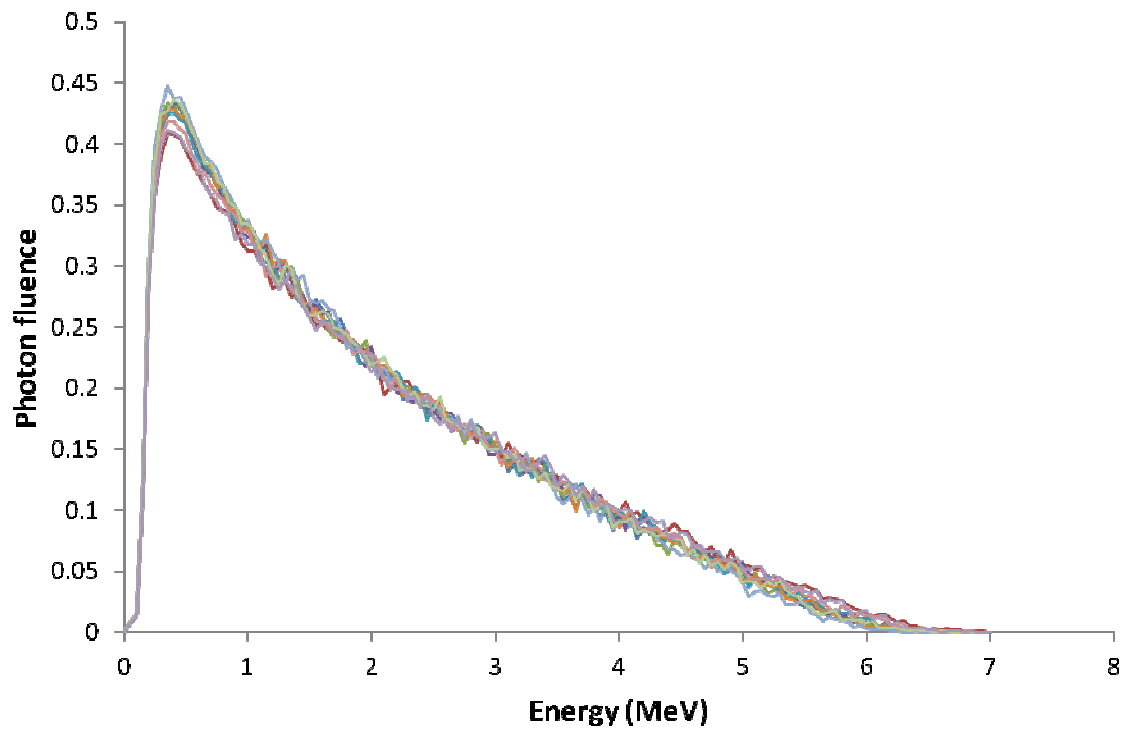


Fig. 5.

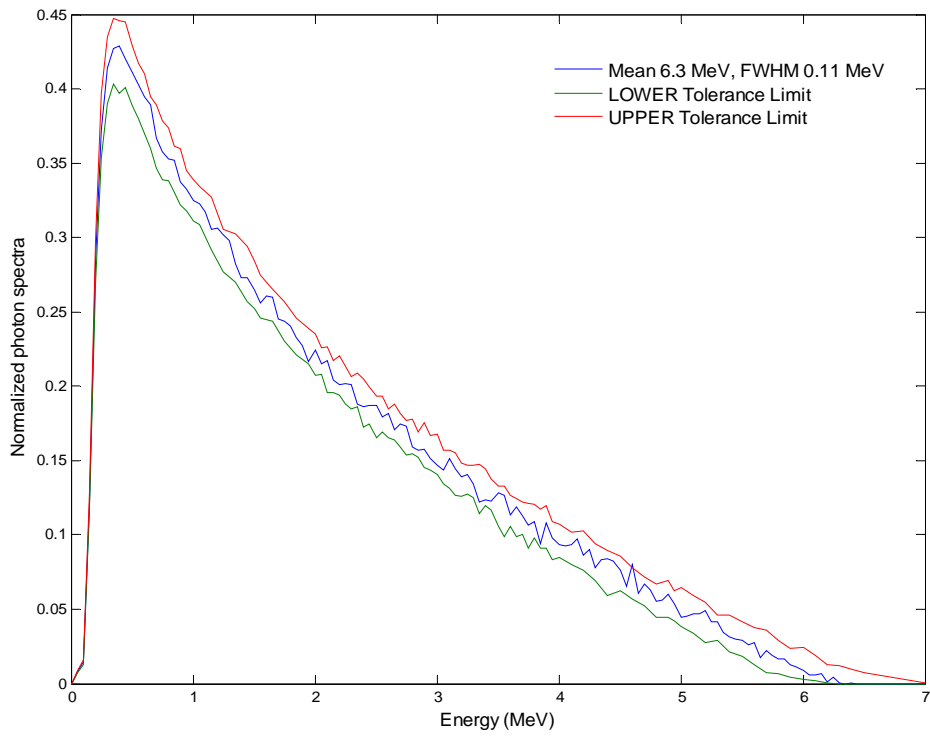


Fig. 6.

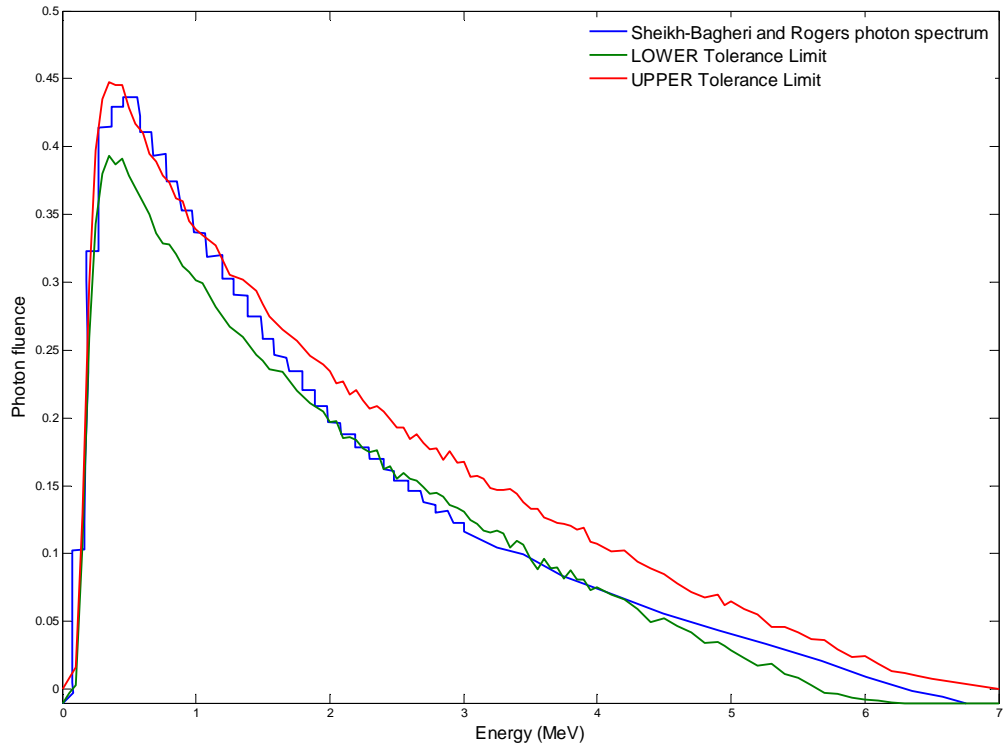


Fig. 7.

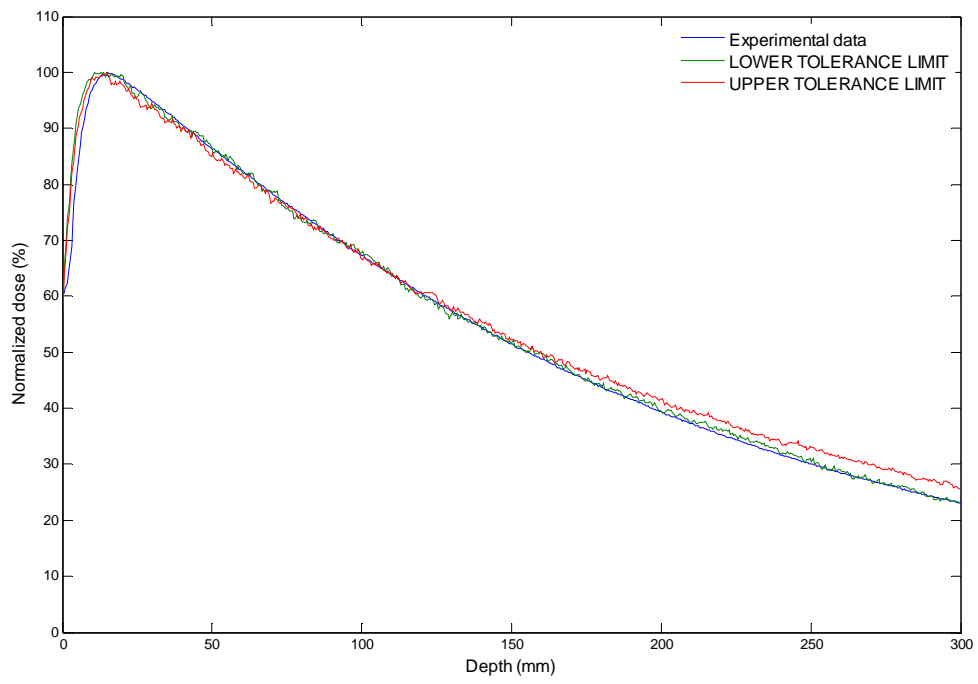


Fig. 8.

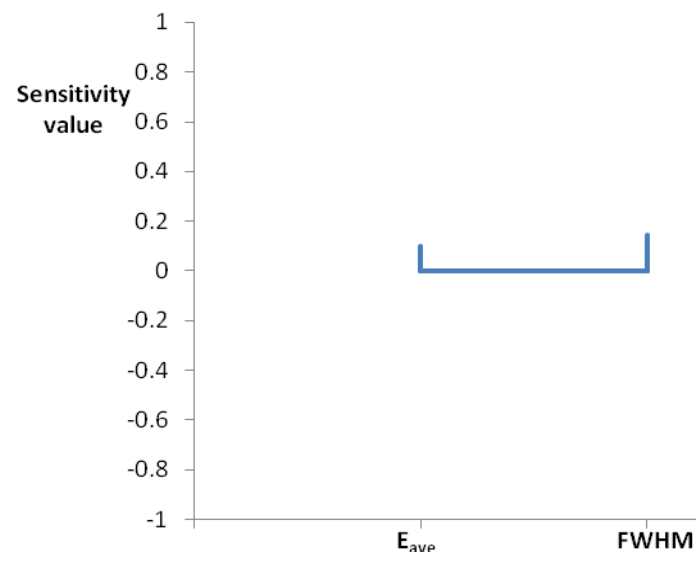


Fig. 9.